

SUPPORTING INFORMATION

***N*-methyl-D-aspartate receptor mediated calcium influx supports *in vitro* differentiation of normal mouse megakaryocytes but proliferation of leukemic cell lines**

Tania Kamal*, Taryn N. Green*, James I. Hearn*, Emma C. Josefsson†‡, Marie-Christine Morel-Kopp§¶, Christopher M. Ward§¶, Matthew J. During***
& **Maggie L. Kalev-Zylinska*††**

* Department of Molecular Medicine & Pathology, University of Auckland, Auckland, New Zealand;

† The Walter and Eliza Hall Institute of Medical Research, 1G Royal Parade, VIC 3052 Australia;

‡ University of Melbourne, Department of Medical Biology, 1G Royal Parade, VIC 3052 Australia;

§ Department of Haematology and Transfusion Medicine, Royal North Shore Hospital, Sydney, Australia;

¶ Northern Blood Research Centre, Kolling Institute, University of Sydney, Sydney, Australia;

** Departments of Molecular Virology, Immunology and Medical Genetics, Neuroscience and Neurological Surgery, Ohio State University, Columbus, OH, USA;

†† LabPlus Haematology, Auckland City Hospital, Auckland, New Zealand.

Correspondence: Dr Maggie L. Kalev-Zylinska, Department of Molecular Medicine & Pathology, University of Auckland, ACM 1142, Auckland, New Zealand.
Tel.: +6421337776; Fax: +6493677121; E-mail: m.kalev@auckland.ac.nz.

Figure S1

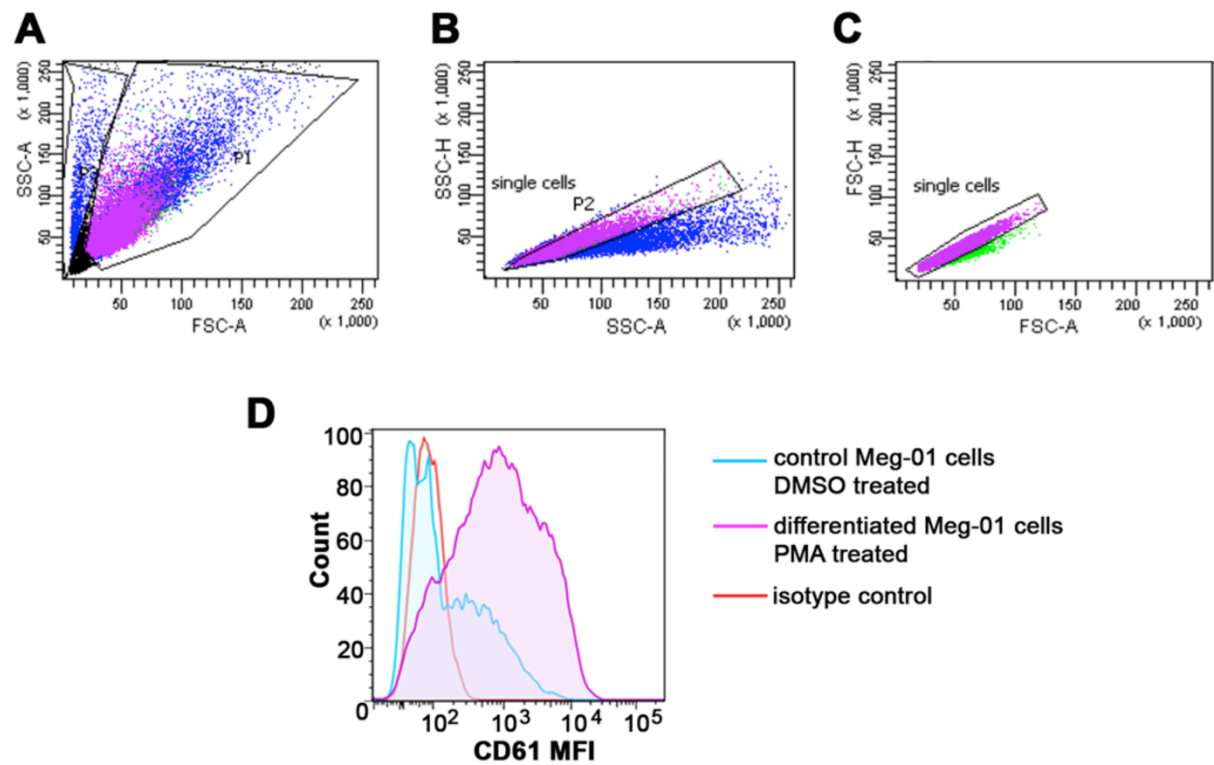


Figure S1. Flow cytometry gating on cultured Meg-01 cells. (A) Single Meg-01 cells were examined based on their forward and side scatter characteristics (FSC-A – SSC-A; pink events). Cell doublets were excluded based on SSC-H – SSC-A (B; blue events) and FSC-H – FSC-A (C; green events). (D) Representative examples of CD61 fluorescence (CD61 MFI using anti-CD61-PE) are shown on Meg-01 cells gated as above. Meg-01 cells were cultured in the presence of 10 nM PMA (differentiated cells; pink line) and 0.1% DMSO (as controls; light blue line); isotype control is shown (red line). Abbreviations: MFI, Mean Fluorescence Intensity; PMA, phorbol-12-myristate-13-acetate.

Figure S2

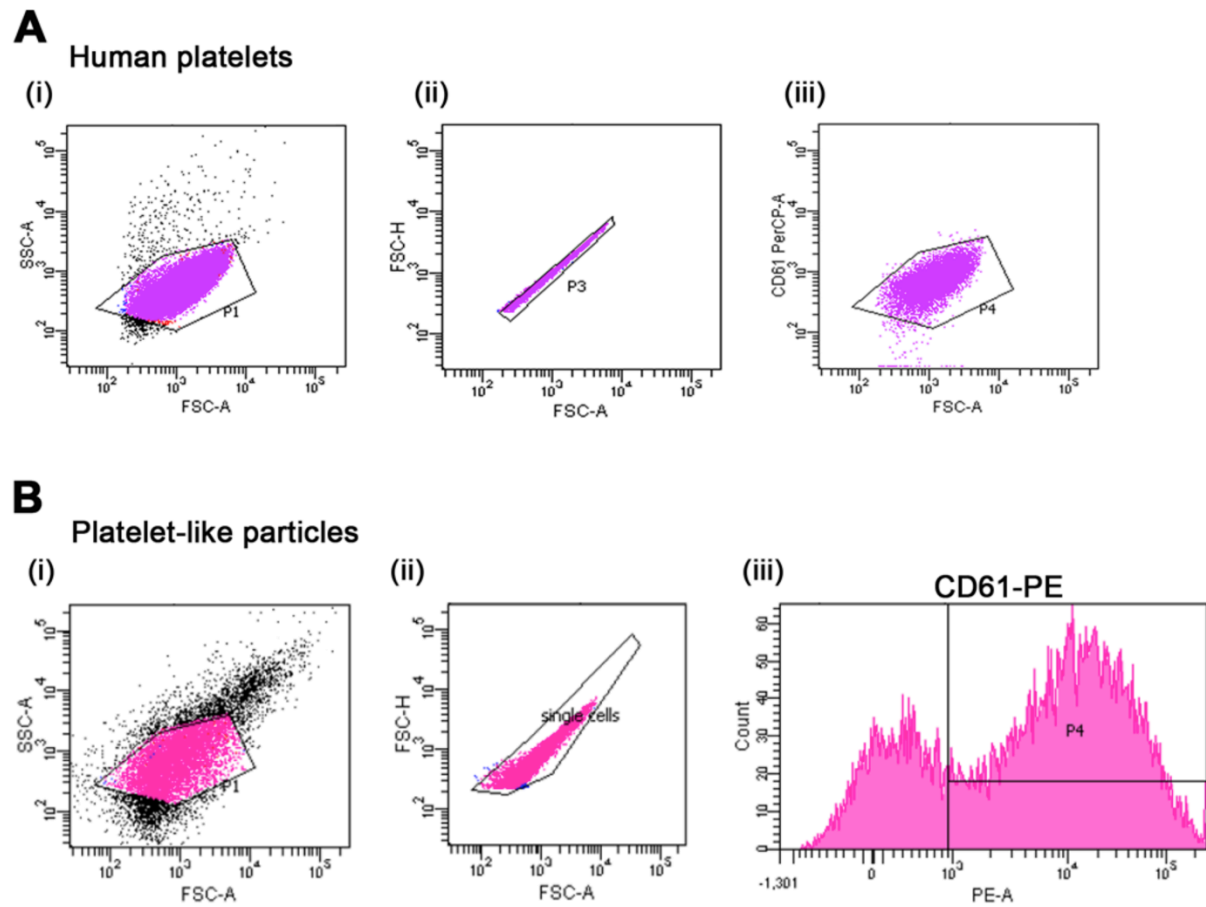


Figure S2. Flow cytometry gating on platelet-like particles. (A) Gates were established based on forward and side scatter characteristics (FSC-A – SSC-A; A.i) of human peripheral blood platelets. Doublets were excluded based on FSC-H – FSC-A (A.ii) and SSC-H – SSC-A (not shown). Gated events were CD61-positive (CD61-PerCP; A.iii). (B) Representative examples of dot plots showing platelet-like particles produced by Meg-01 cells acquired using the gate established in A. Meg-01 cells in this example were cultured in the presence of 500 μ M valproic acid. Forward and side scatter characteristics (B.i), the exclusion of doublets from FSC-H – FSC-A (B.ii) and CD61 expression levels (CD61-PE; B.iii) are shown.

Figure S3

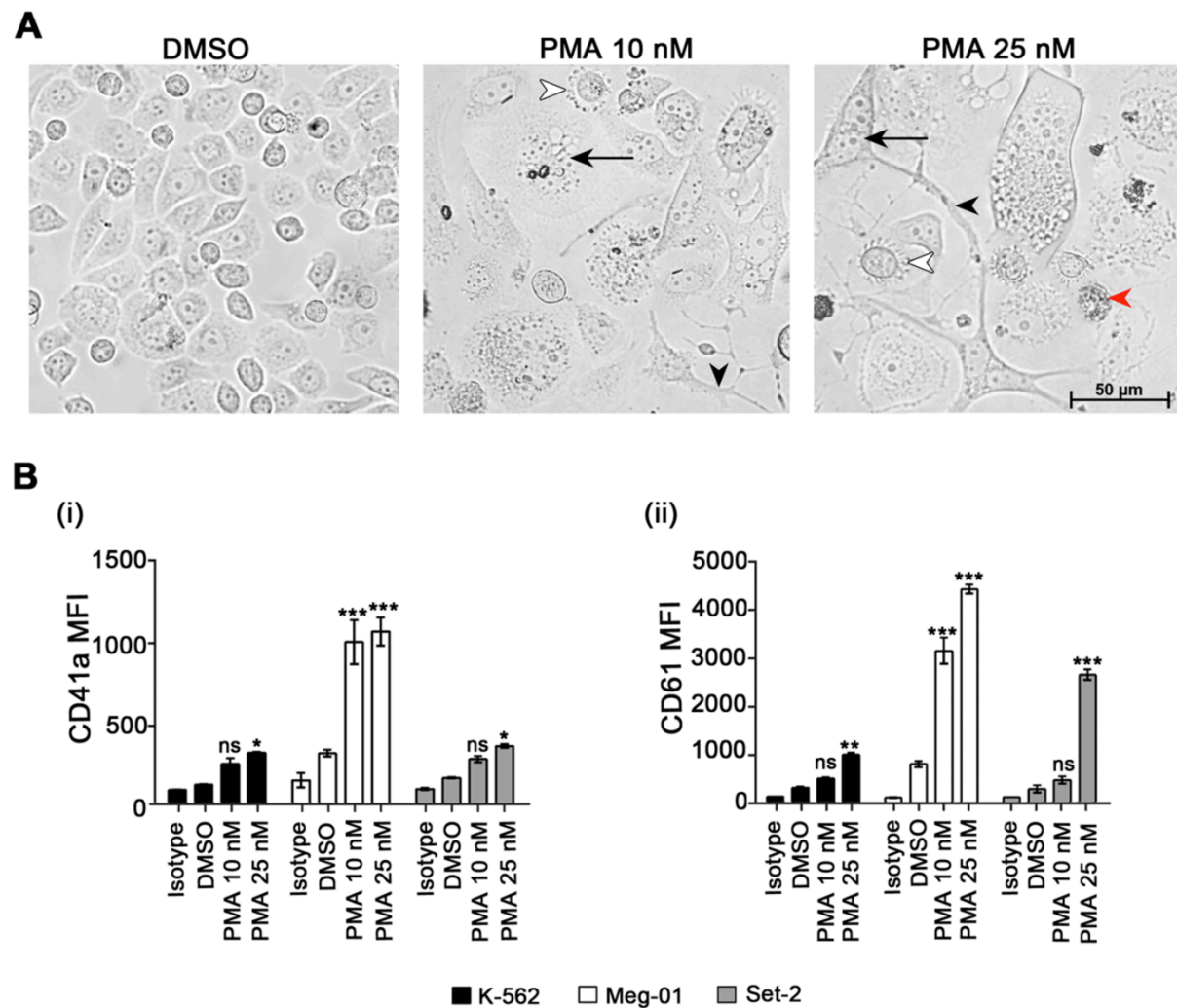


Figure S3. PMA model of Meg-01 cells differentiation. (A) Representative morphology of Meg-01 cells cultured for 3 days in the presence of 10 and 25 nM PMA or 0.1% DMSO control, as indicated. PMA increased formation of proplatelet-like cytoplasmic extensions (black arrowheads), budding of platelet-like particles (white arrowheads) and nuclear lobulation (black arrows). Features of differentiation were stronger at 25 nM PMA but cell degeneration was also more common under these conditions (red arrowhead). Live cells were imaged under phase contrast after 3 days in culture. Scale bar, 50 μ M for all. (B) Expression of CD41a (B.i) and CD61 (B.ii) antigens on K-562, Meg-01 and Set-2 cells determined by flow cytometry after 3 days in culture. Data are mean \pm SEM for the MFI from two

independent experiments. The level of statistical significance is shown compared with the DMSO control (* $P < 0.05$; ** $P < 0.01$; *** $P < 0.001$; ns, non-significant; one-way ANOVA with Dunnett's *post-hoc*). Abbreviations: DMSO, dimethyl sulfoxide; MFI, Mean Fluorescence Intensity; PMA, phorbol-12-myristate-13-acetate.

Figure S4

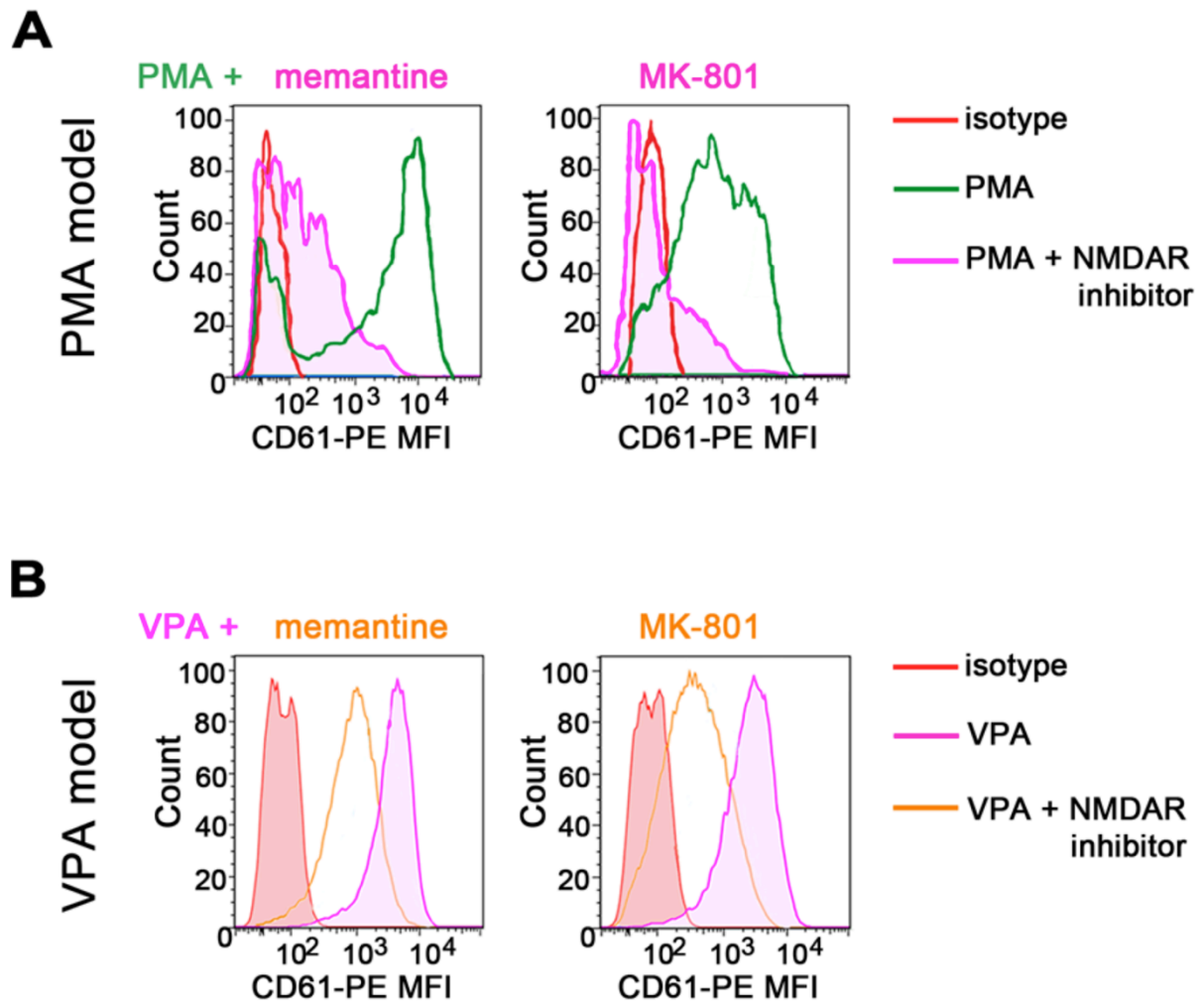


Figure S4. Flow cytometric histogram examples demonstrating an effect of NMDAR antagonists on PMA and VPA induced differentiation of Meg-01 cells. Meg-01 cells were differentiated using 10 nM PMA over 3 days (A) and 500 μ M VPA over 7 days (B). Effects of memantine and MK-801 were tested at 100 μ M. CD61 expression was examined using anti-CD61-PE. Representative histogram examples are shown demonstrating expression of CD61 (CD61 MFI), including cell counts and isotype controls. The addition of NMDAR antagonists reduced expression of CD61 driven by both PMA (in A) and VPA (in B). Abbreviations: MFI, Mean Fluorescence Intensity; PMA, phorbol-12-myristate-13-acetate; VPA, valproic acid.

Figure S5

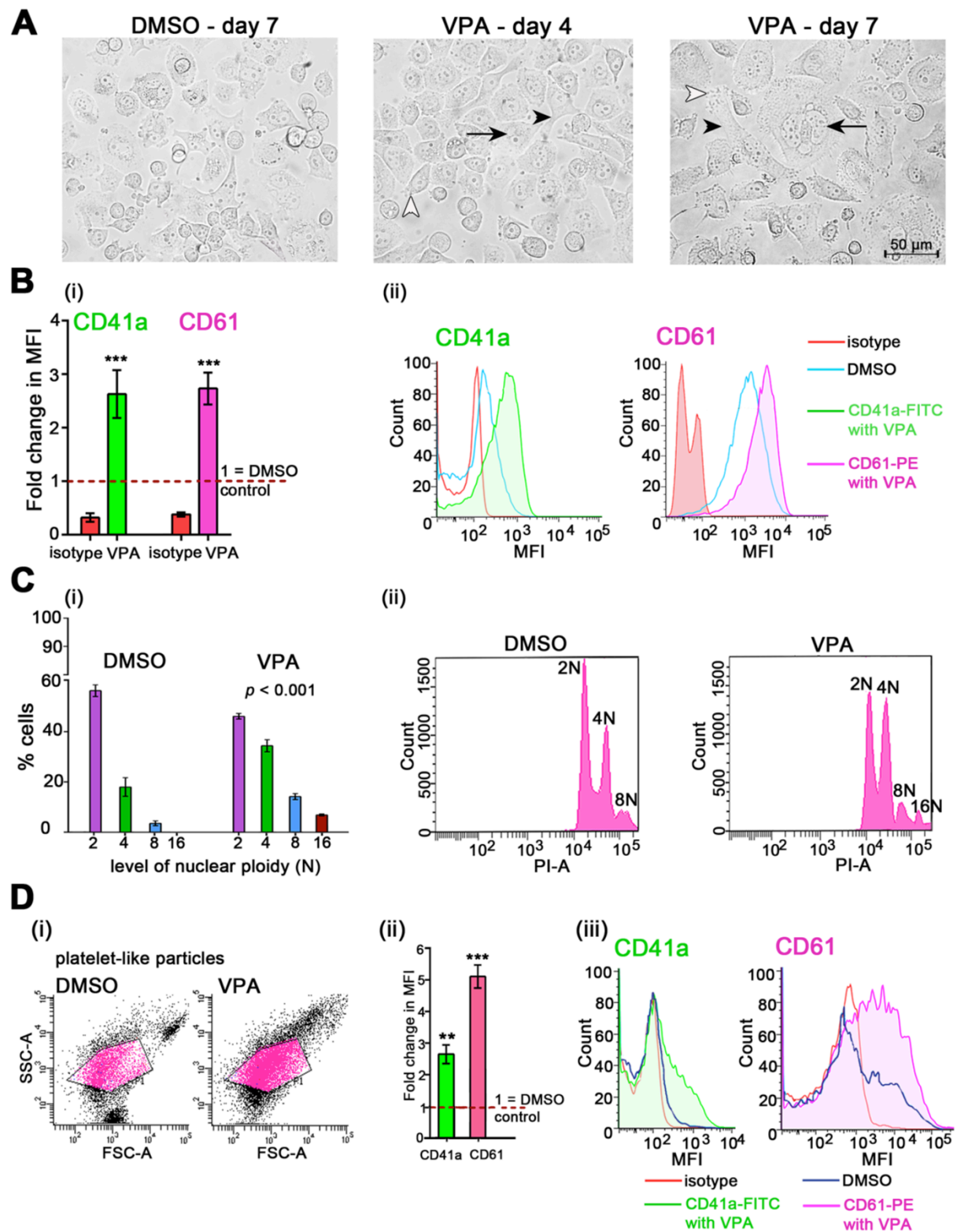


Figure S5. VPA model of Meg-01 cells differentiation. Meg-01 cells were cultured for 7 days in the presence of 500 μ M VPA or 01.% DMSO control. (A) Live cells were imaged under phase contrast, and representative morphology is shown on days 4 and 7, as indicated. In the presence of VPA, cells were larger and healthier-looking than with DMSO. VPA increased formation of proplatelet-like cytoplasmic extensions (black arrowheads), budding of platelet-like particles (white arrowheads) and nuclear lobulation (black arrows). Scale bar, 50 μ M for all. (B) Expression of CD41a and CD61 on Meg-01 cells cultured in the presence of VPA and controls determined by flow cytometry. Bars in B.i demonstrate a fold change in expression shown as mean \pm SEM of the MFI. Representative overlay histograms are shown in B.ii. (C) Nuclear ploidy of Meg-01 cells under conditions indicated. Bars in C.i demonstrate the level of ploidy shown as mean \pm SEM; 2, 4, 8 and 16 N indicate ploidy classes. Representative examples of ploidy plots are shown in C.ii. (D) Production of platelet-like particles by Meg-01 cells in the presence of VPA examined by flow cytometry. Representative examples of dot plots are shown in D.i. Bar graphs in D.ii demonstrate a fold change in the numbers of platelet-like particles determined from CD41a and CD61 expression; representative examples of overlay histograms are shown in D.iii. All graphed data are mean \pm SEM from three independent experiments. The level of statistical significance is shown compared with the DMSO control (** $P < 0.01$; *** $P < 0.001$). Ploidy data was analyzed by two-way ANOVA with Bonferroni correction for multiple comparisons; other data by one-way ANOVA with Dunnett's *post-hoc*. Abbreviations: DMSO, dimethyl sulfoxide; MFI, Mean Fluorescence Intensity; ns, non-significant; PI, propidium iodide; VPA, valproic acid.

Figure S6

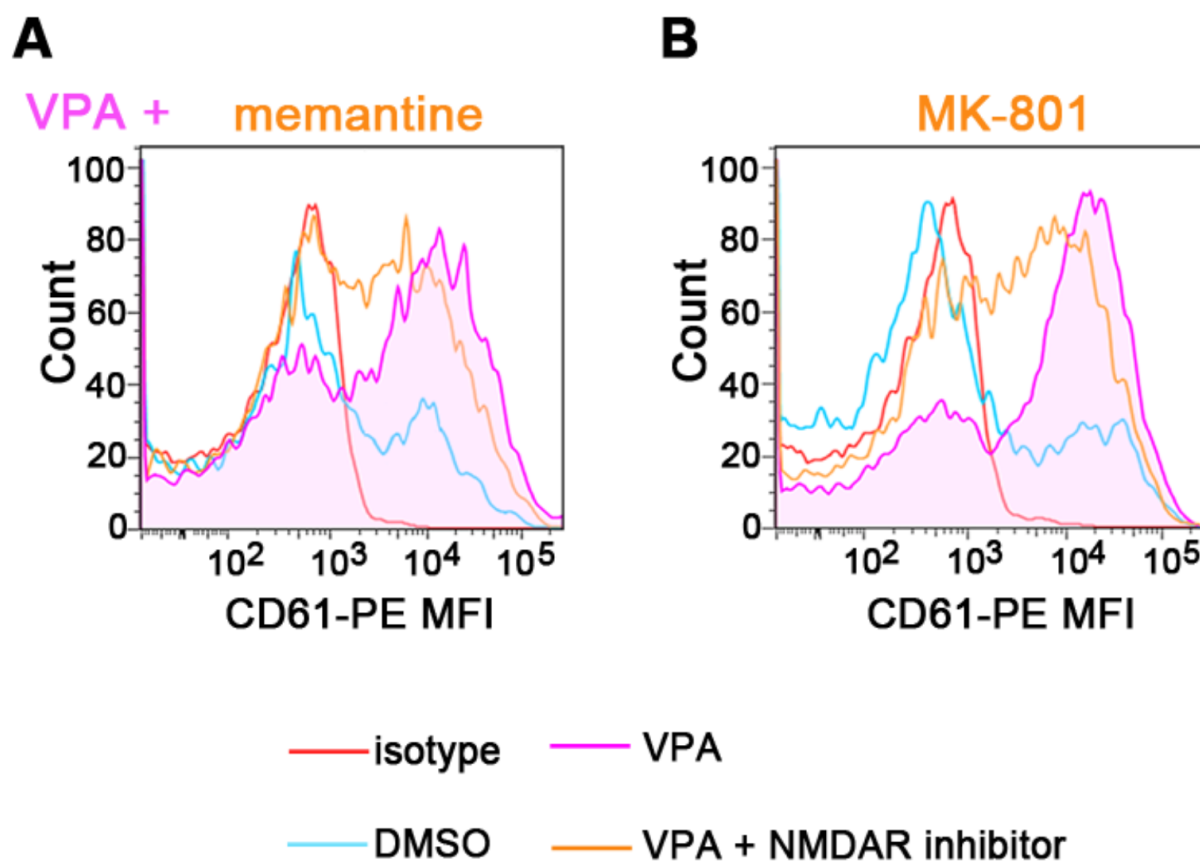


Figure S6. Flow cytometric histogram examples demonstrating an effect of NMDAR antagonists on the release of platelet-like particles from Meg-01 cells. Meg-01 cells were cultured for 7 days in the presence of valproic acid (VPA; 500 μ M) without or with NMDAR antagonists (memantine and MK-801; 100 μ M). At the end of cultures, media samples were collected and spun to enrich for platelet-like particles; these were examined using gates established by testing of human peripheral blood platelets (see Figure S2). Representative histogram examples are shown demonstrating that memantine and MK-801 reduced the number of CD61-positive particles released from Meg-01 cells driven by VPA. Quantitative data from repeat experiments are shown in Figure 1D. Abbreviations: DMSO, dimethyl sulfoxide; MFI, Mean Fluorescence Intensity; VPA, valproic acid.

Figure S7

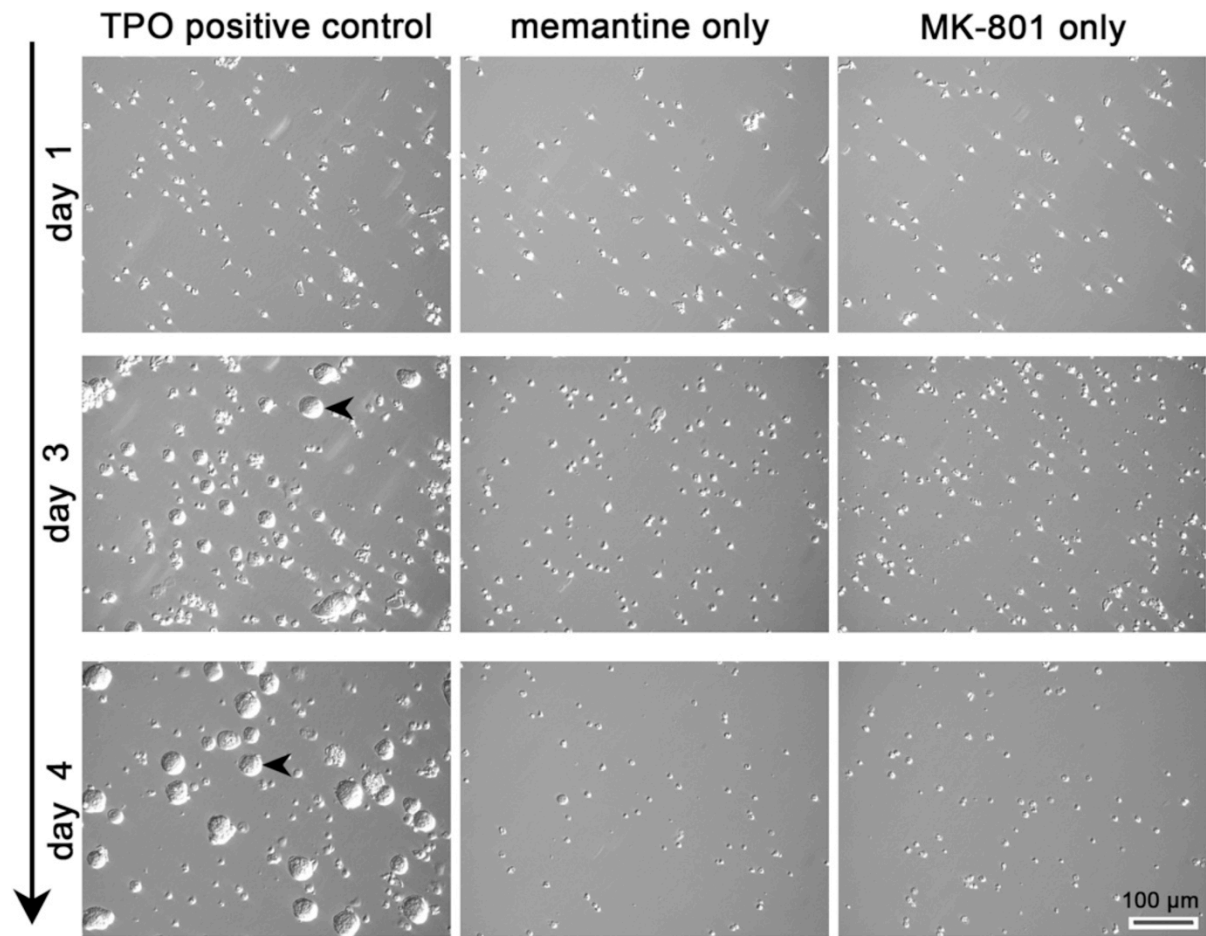


Figure S7. NMDAR antagonists by themselves are not sufficient to induce megakaryocytic differentiation of lineage-negative progenitors. Lineage-negative progenitors were isolated from mouse marrow and cultured for 4 days in SFEM II media in the presence of: (A) 40 nM thrombopoietin (TPO); (B) 100 μ M memantine; (C) 100 μ M MK-801; with no TPO added in B and C. Morphological features of live cells are shown using phase-contrast photomicrographs taken on days 1, 3 and 4 of cultures; images are representative of three independent experiments. TPO induced strong megakaryocytic differentiation over 4 days; black arrows point to examples of large, differentiated cells. In contrast, when memantine and MK-801 were applied in the absence of TPO, cells remained small and spherical. Scale bar, 100 μ m for all.

Figure S8

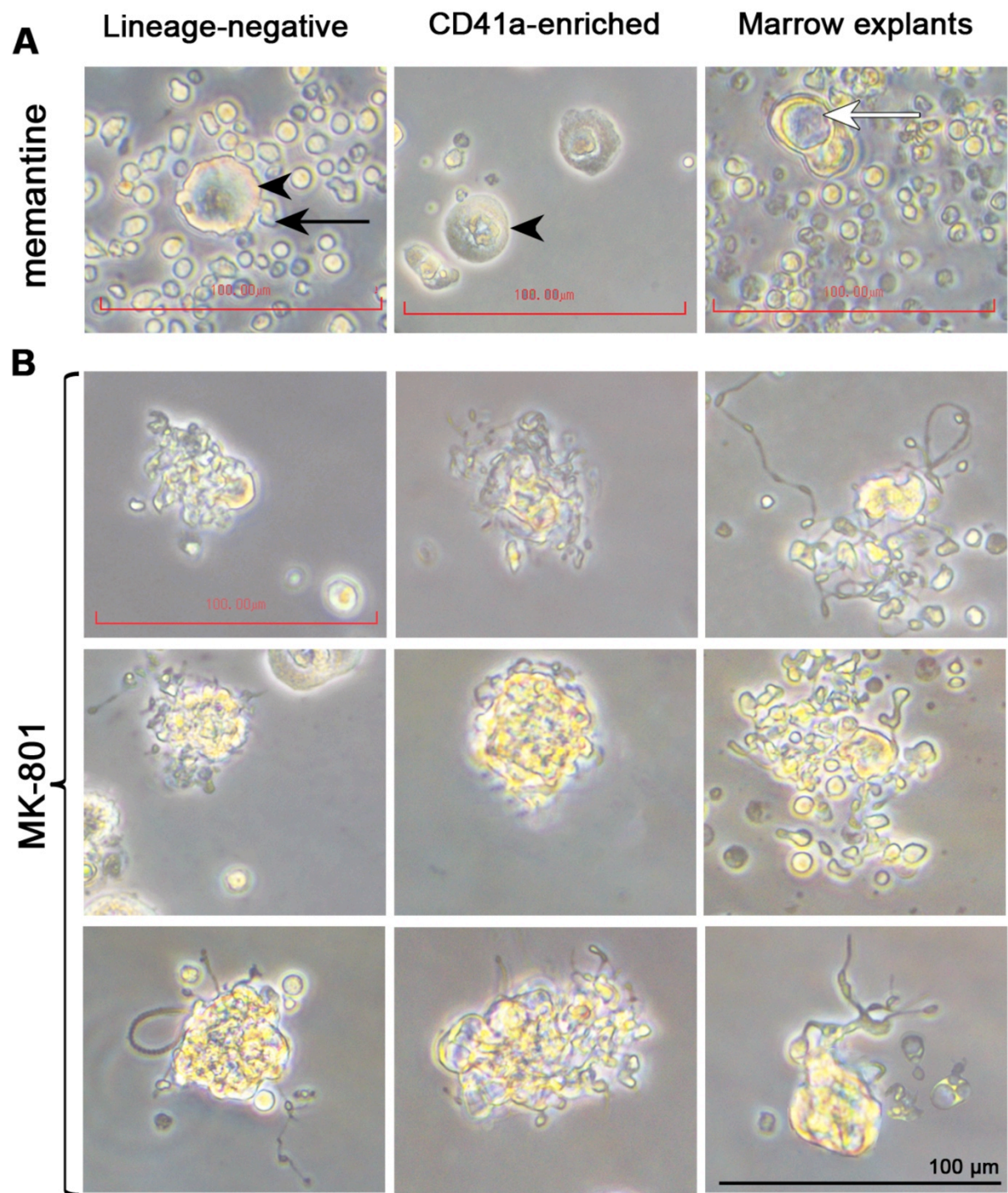


Figure S8. Gallery of images demonstrating defects in proplatelet formation induced by NMDAR antagonists in mouse megakaryocytes. Megakaryocytes were cultured in the presence of: (A) memantine, (B) MK-801 (both at 100 μM) from lineage-negative progenitors, CD41a-enriched precursors and bone marrow explants, as indicated. Exogenous

thrombopoietin was added to lineage-negative and CD41a-enriched cultures. In all culture types, memantine markedly inhibited proplatelet formation, and most cells remained spherical (black arrowheads). Rare broad cytoplasmic protrusions were seen (black arrow) as well as cytoplasmic vacuoles (white arrow). (B) Rare proplatelets that developed in the presence of MK-801 were short, disorganized and often looping. Phase-contrast photomicrographs were taken from a range of cultures as shown, all of which were performed at least in three independent experiments. Proplatelet defects were virtually identical between all culture types. Scale bars, 100 μ m for all.

Figure S9

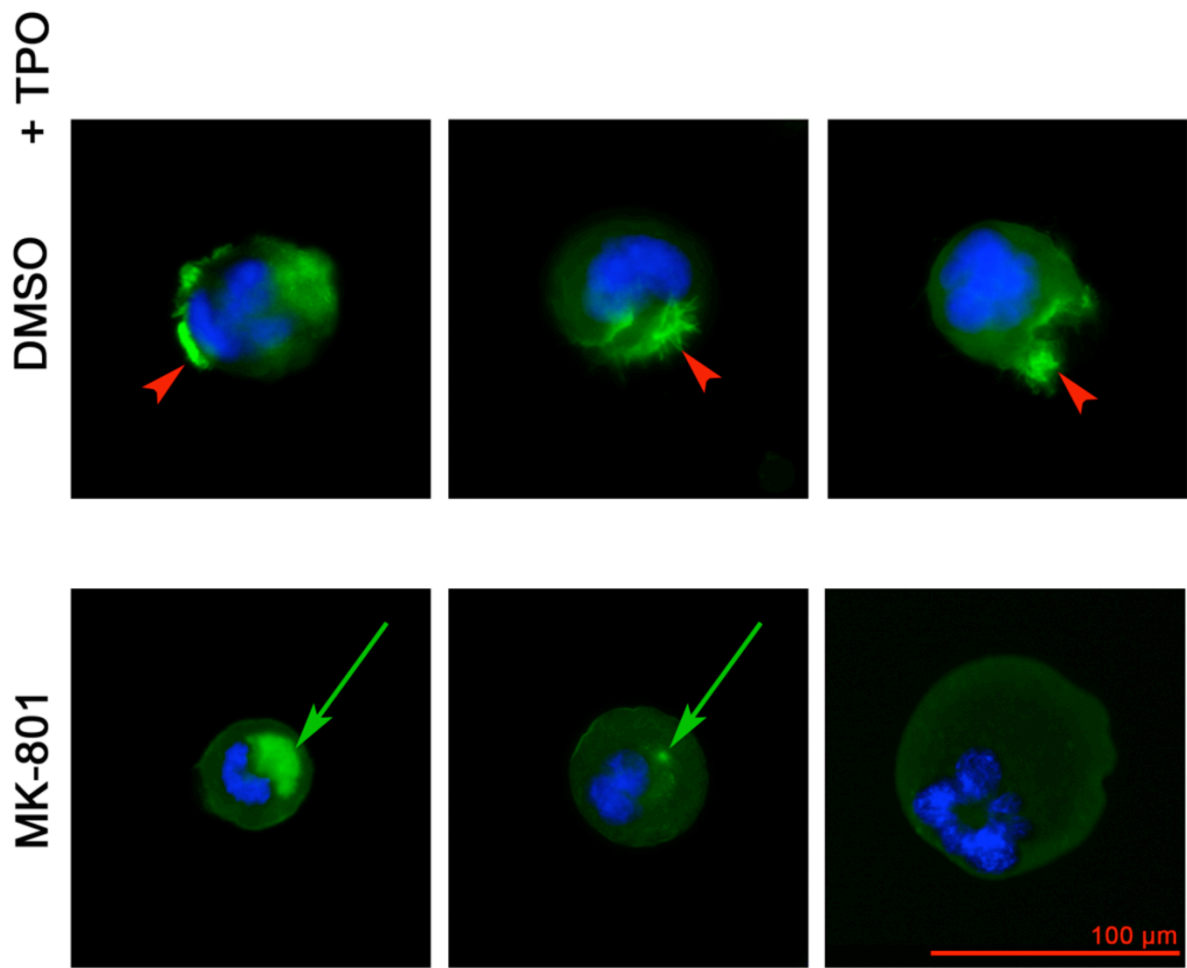


Figure S9. Impaired reorganization of actin in the presence of MK-801. Mouse lineage-negative progenitors were cultured in the presence of 40 nM thrombopoietin (TPO) without and with 100 μ M MK-801. 0.1% DMSO was applied to control wells. On day 5, mature megakaryocytes were enriched on Percoll gradient and stained with Alexa FluorTM 488 Phalloidin to visualize filamentous actin (F-actin). Nuclei were counterstained using Hoechst 33258. Red arrowheads point to the formation of focal complexes of F-actin frequently seen in control megakaryocytes. On the other hand, megakaryocytes cultured in the presence of MK-801 showed mostly intracellular staining deposits (green arrows). Representative images are shown taken with a Nikon Eclipse Ti-U inverted microscope. Scale bar, 100 μ m for all.